

**Theoretical investigation on the kinetics of dimethyl phosphoramidate with hydroxyl radicals**

Şeyda Aydogdu and Arzu Hatipoglu*

Department of Chemistry, Yildiz Technical University, 34220 Istanbul, Turkey

E-mail: hatiparzu@yahoo.com

Manuscript received online 26 April 2019, revised and accepted 20 July 2019

In this paper the reaction kinetics of dimethyl phosphoramidate with hydroxyl radical was investigated with Density Functional Theory. Geometry optimization and energy calculations of the reactants, the pre-reactive complexes, the transition states and the products were performed at the B3LYP/6-31G(d) basis set. The water effect was computed by using CPCM as the solvation model. Rate constants of all the possible reaction paths were calculated via Transition State Theory. The branching ratio for each of the reaction paths was calculated. The most probable reaction path was found the hydrogen abstraction from methyl group of dimethyl phosphoramidate.

Keywords: Dimethyl phosphoramidate, •OH radical, DFT, rate constant, aqueous medium.

Introduction

Organophosphorus compounds are those having at least one phosphorus atom bonded to carbon atom. Phosphoramidate is an important class of organophosphorus compounds¹. This class is characterized by possessing one amino functional group bonded to phosphorus atom in their structure². They are used in different areas such as insecticides, flame retardant, lubricating oil additives and in medicine industry as an antitumor¹⁻³. As a consequence of increasing use over time, they have found in different environmental counterparts⁴. They transport to atmosphere and also reach aqueous resources from different process. The persistence of them in aqueous environment have a public concern because of their toxic character^{4,5}. Hence, removal of these compounds from the environment is a necessary task. Therefore, there is a need to remove these compounds from the environment.

Hydroxyl radical has the major role in the degradation reactions of organic pollutants⁶. Therefore, mechanism and kinetics of the degradation reactions of organic pollutants with •OH radical are important. However, limited information is available on the phosphoramidates degradation reaction mechanism. There are some experimental kinetic studies in the literature about phosphoramidates. Sun *et al.* have in-

vestigated the photocatalytic decomposition of diethyl phosphoramidate (DEPA) over TiO₂. They examined that the parameters like pH, reactant concentration, TiO₂ concentration and temperature that affected to the reaction kinetics of DEPA⁷. Photocatalytic oxidation of some organophosphorus compounds in water TiO₂ suspension studied by some researchers^{8,9} and they observed that oxidation mainly proceeded through the α carbon atom. Although, it is not possible to understand the reaction mechanism or product distribution from these studies. Product distribution of a reaction is also important to predict the detailed reaction mechanism and relative importance of each reaction paths^{10,11}.

The important problem in kinetic studies is to determine intermediates because of their short lifetime. Moreover, sometimes intermediates are more toxic than reactants¹². For these reasons theoretical calculation methods can be suitable alternatives. Indeed, these methods can offer necessary informations on the reaction mechanism, products and intermediates¹³. As far as we know, there is no experimental or theoretical study about the reaction of dimethyl phosphoramidate with •OH radical. The aim of this study to determine the reaction mechanism of DMP with •OH radical. For this purpose rate constants and product distributions of all the possible reaction paths were calculated in gas phase and aqueous medium.

Computational method

In this study, DMP and hydroxyl radical reaction was investigated theoretically. Geometry optimizations of the reactants, the product radicals, the pre-reactive and the transition state complexes were performed with the Density Functional Theory (DFT) method within the GAUSSIAN 09 package¹⁴. DFT calculations were performed with B3LYP method which combines HF and Becke exchange term with Lee-Yang-Parr correlation functional with 6-31G(d) as the basis set^{15,16}. The forming bonds were chosen as reaction coordinate in determining the transition states structures. All the stationary states were confirmed by having real frequencies whereas transition states have only one imaginary frequency that related to reaction coordinate^{12,17}. Intrinsic Reaction Coordinate (IRC) calculations have been performed in order to verify the connections of transition states to true reactant and products¹⁸. The solvent effect on the reaction was taken into account using CPCM (the conductor-like polarizable continuum model) as the solvation method. The solvent was water with the dielectric constant value $\epsilon = 78.39$. In this method, solute molecule is placed in a cavity that surrounded by solvent molecule¹⁹.

Results and discussion

Product radicals, pre-reactive and transition state complexes:

The hydroxyl radical is a very active species and has an electrophilic character²⁰. In this study the four possible reaction pathways investigated for the DMP with $\bullet\text{OH}$ radical reaction are given in the Fig. 1. Based on the literature search, the $\bullet\text{OH}$ radicals react with DMP four different ways²¹. The $\bullet\text{OH}$ radicals react with hydrocarbons through H-abstraction and it is a simple atom transfer reaction¹². In this reaction two different hydrogen can be abstracted by hydroxyl radical. The first one, from methyl group (Path 1) and the second one from amino group (Path 2). For these paths one of the C-H or N-H bond is broken and a new bond is formed to the oxygen atom of $\bullet\text{OH}$ radical. Another feasible reaction way is $\bullet\text{OH}$ radical attack to the double bond of the P atom of P=O group (Path 3). The fourth reaction pathway is, O-CH₃ bond cleavage, $\bullet\text{OH}$ radical bound to CH₃ group to form CH₃OH as a product (Path 4).

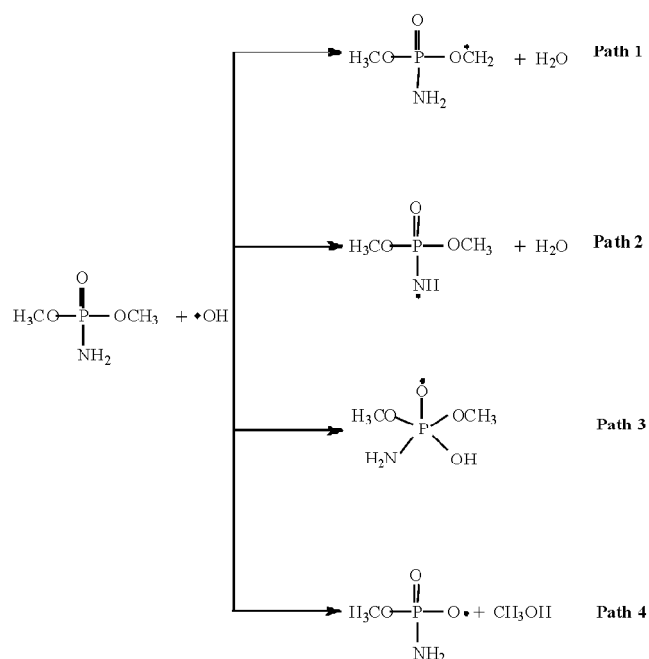


Fig. 1. Possible reaction paths for the DMP + $\bullet\text{OH}$ reaction.

Four different radicals were determined as the products of the reaction between DMP and $\bullet\text{OH}$ radical. Potential energy profile of the modeled reaction mechanism with the structures of the optimized radical products were represented in Fig. 2(a) and (b) for gas phase and aqueous medium respectively. As seen in Fig. 2 the most stable product radical was R1 whose energy was 5.70, 21.47 and 20.64 kcal mol⁻¹ less than the R2, R3 and R4 respectively. The same sequence was observed for aqueous medium. It may be concluded that R1 was the most probable radical by using Wheland localization approach²². R1 and R2 radicals are more stable in aqueous medium. This was attributed to the hydrogen bond stabilization between the water molecules and product radicals. The stabilities of the product radicals increase by ca. 9.51 kcal mol⁻¹ in aqueous medium.

It has been demonstrated that, weakly bound complexes were formed between the $\bullet\text{OH}$ radical and DMP. These complexes are pre-reactive complexes. Because of these complexes the reaction pathways which being investigated proceed through lower energy barrier than the reagents¹². For the DMP with $\bullet\text{OH}$ radical reaction two different pre-reactive complexes PC1 and PC2 were determined due to the literature search. There is no pre-reactive complexes for Path 3

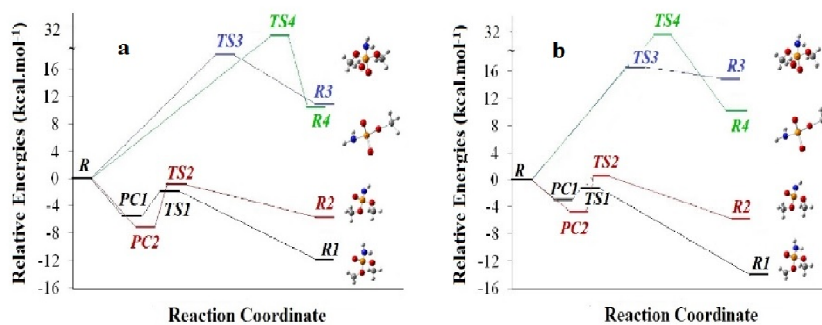


Fig. 2. Potential energy diagram for the reaction of DMP with $\bullet\text{OH}$ radical for (a) gas phase and (b) aqueous medium.

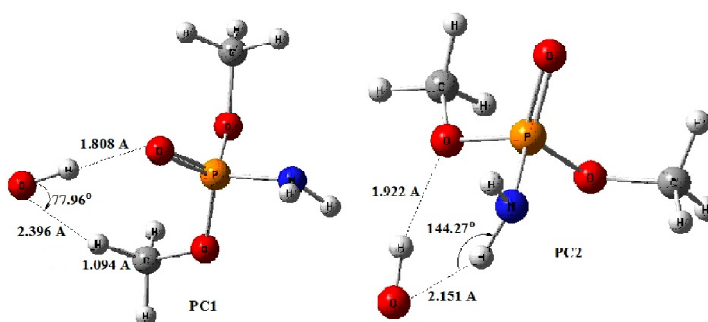


Fig. 3. The optimized structures of the pre-reactive complexes.

and 4 due to higher energies of TS complexes than reactants. This pathways were energetically unfavorable²³. The structure of pre-reactive complexes of DMP with $\bullet\text{OH}$ radical reaction were presented in Fig. 3. The $\bullet\text{OH}$ radical is seen to approach the hydrogen atom almost 79° in the abstraction paths. The main difference in the optimized geometries occurs in the distance between the oxygen atom of $\bullet\text{OH}$ and the hydrogen atom that being abstracted. This distance were 2.396 Å for PC1 and 2.151 Å for PC2. Energetically PC2 was more stable than PC1 in both phases. PC1 and PC2 were lying 5.46 and 7.19 kcal mol⁻¹ below isolated reactants respectively. The PC2's energy was 1.73 kcal mol⁻¹ below than PC1. In aqueous media the same sequence was observed.

Four transition states TS1, TS2, TS3 and TS4 were determined for the possible reaction paths. The optimized structures of the transition states were given in Fig. 4. In the abstraction reaction paths (Path 1 and 2) $\bullet\text{OH}$ radicals approach one of the hydrogen atom of DMP to form an O-H bond while the C-H or N-H bonds are broken. The considerable changes

in the geometry of DMP are localized around the hydrogen atom being abstracted the carbon atom (TS1) or nitrogen atom (TS2) in the transition state complexes. The breaking bond is lengthening the others stay the same. The lengthening of the C-H and N-H bonds were 0.15 Å and 0.12 Å respectively for TS1 and TS2. In the structure of TS3 and TS4 newly occurring bond distances were 1.659 Å (O-P) and 1.793 Å (C-O) respectively. Elongation of occurring bond lengths of TS3 and TS4 were 0.178 Å, 0.355 Å respectively. Furthermore, TS1 has the lowest total energy as seen in Fig. 2 that is indicating that TS1 most energetically stable one. TS1 structure was energetically 0.42, 20.76 and 33.85 kcal mol⁻¹ more stable than TS2, TS3 and TS4. The energies of transition state structures TS1 and TS2 were *ca.* 2.65 kcal mol⁻¹ below the reactants whereas the energies of TS3 and TS4 were *ca.* 24.45 kcal mol⁻¹ higher the reactants. In aqueous medium energies of TS1 lied 1.66 kcal mol⁻¹ below the reactants, whereas TS2, TS3 and TS4 were 0.55, 15.66, 31.85 kcal mol⁻¹ above the reactants. All the transition states were verified with having only one imaginary frequency that corre-

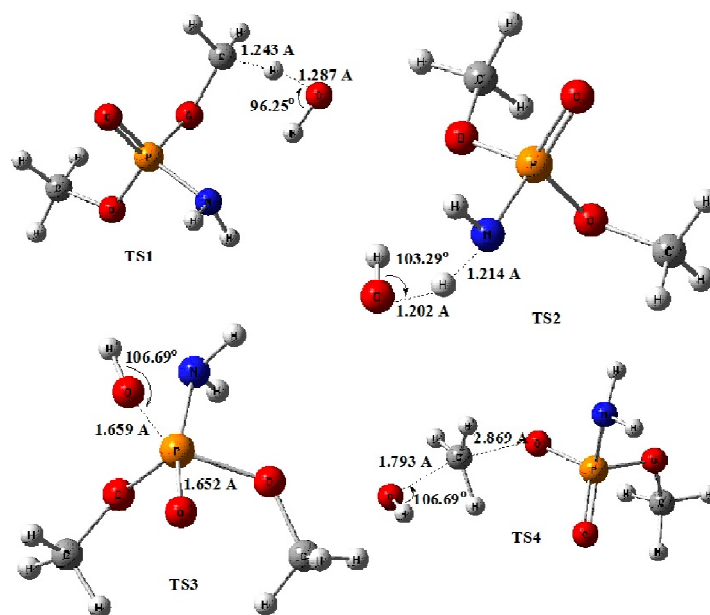


Fig. 4. The optimized structures of the transition states.

sponding the reaction coordinates. In the studied reaction the imaginary frequencies of TS1, TS2, TS3 and TS4 were $1269i$, $1555i$, $268i$ and $965i$ cm^{-1} for gas phase ($1283i$, $1599i$, $141i$ and $954i$ cm^{-1} for aqueous medium). Transition states were also confirmed by IRC calculations, too.

Energetic and reaction constants of reaction paths:

Enthalpy and Gibbs free energy changes for the possible reaction paths were listed in Table 1. As seen in table Path 1 and 2 reaction paths were exothermic and exergonic. Since the Gibbs free energies had negative values, it may be concluded that reactions Path 1 and 2 were thermodynamically favored in both phases. The highest exothermicity was belong to Path 1 in gas phase and aqueous medium. Further-

Table 1. Enthalpy and Gibbs free energy changes for the possible reaction paths at 298.15 K

| | Gas phase | | Aqueous medium | |
|--------|--|--|--|--|
| | ΔH (kcal mol^{-1}) | ΔG (kcal mol^{-1}) | ΔH (kcal mol^{-1}) | ΔG (kcal mol^{-1}) |
| Path 1 | -7.86 | -12.44 | -12.84 | -13.98 |
| Path 2 | -1.92 | -6.80 | -6.18 | -7.46 |
| Path 3 | 17.97 | 33.50 | 14.42 | 38.12 |
| Path 4 | 56.37 | 33.66 | 53.49 | 32.34 |

more, this study revealed that Path 3 and 4 were unfavorable because of the their high reaction barriers.

The calculated activation energies for the reaction of DMP with $\bullet\text{OH}$ radical were given in Table 2. As seen in the Table

Table 2. Activation energies, rate constants and product distributions for the DMP + $\bullet\text{OH}$ reaction at 298.15 K

| | Path 1 | Path 2 | Path 3 | Path 4 |
|---|-----------------------|------------------------|------------------------|------------------------|
| Gas phase: | | | | |
| E_a (kcal mol^{-1}) | 2.60 | 4.74 | 17.97 | 30.98 |
| k ($\text{cm}^3 \text{molec}^{-1} \text{s}^{-1}$) | 1.38×10^{-9} | 9.81×10^{-10} | 3.09×10^{-26} | 1.64×10^{-30} |
| Branching ratio (%) | 58.47 | 41.57 | 1.30×10^{-15} | 6.95×10^{-20} |
| Aqueous medium: | | | | |
| E_a (kcal mol^{-1}) | 1.95 | 4.80 | 15.66 | 31.85 |
| k ($\text{cm}^3 \text{molec}^{-1} \text{s}^{-1}$) | 5.43×10^{-9} | 3.58×10^{-9} | 3.69×10^{-23} | 9.29×10^{-31} |
| Branching ratio (%) | 60.27 | 39.73 | 4.09×10^{-13} | 1.03×10^{-20} |

2 the activation energy of Path 1 was the lowest in both gas phase and aqueous medium. Activation energies of Path 2, Path 3 and Path 4 were 2.14, 15.37 and 28.38 kcal mol⁻¹ higher than Path 1 in gas phase (2.85, 13.71 and 29.90 kcal mol⁻¹ higher in aqueous medium). The values in Table 2 showed that activation energies in aqueous medium was reduced by 0.65 and 2.31 kcal mol⁻¹ for Path 1 and Path 3. However the activation energy of Path 2 and Path 4 were 0.06 and 0.87 kcal mol⁻¹ higher in aqueous medium than in gas phase.

The rate constants for the all of the paths were calculated by Transition State Theory at 298.15 K²⁴. The rate constants are calculated by using below equation,

$$k = \frac{k_B T}{h} \frac{q_{TS}}{q_{OH} q_{DMP}} e^{-E_a/RT}$$

in this equation k_B is Boltzman's constant, h is Planck's constant, T is temperature, E_a is the activation energy and q_{TS} , q_{DMP} and q_{OH} are the molecular partition functions for transition state, DMP and •OH radical respectively. Rate constant of the each paths were calculated by Transition State Theory and obtained results were summarized in Table 2. The Path 1 had the highest rate constant followed by Path 2, 3 and 4 in gas phase. The rate constant squence was same in aqueous medium. The rate constants for reaction paths were more fast in aqueous medium than gas phase because of the hydrogen bond stabilization. The branching ratio for each of the reaction paths was calculated and presented in Table 2. By using the branching ratio the dominant reaction path was Path 1 for both phases.

Calculated overall rate constants value were 2.36×10^{-9} and 9.01×10^{-9} cm³ molec⁻¹ s⁻¹ for gas phase and aqueous medium respectively. Rate constant values, activation energies and branching ratio values were in accordance. From the obtained activation energies and rate constant results it could be concluded that the hydrogen abstraction from methyl group was prevail path (Path 1) in both phases.

Conclusions

In this study, reaction kinetics for the reaction of DMP with •OH radical were investigated theoretically both in gas phase and aqueous medium. On the basis of DFT calcula-

tions four different reaction paths have been determined for the reaction. The hydrogen abstraction complexes are early transition states while addition complexes are late complexes on the reaction coordinate. The most probable reaction path was hydrogen abstraction from the methyl group (Path 1). This path had a low activation energy barrier and was also energetically most favourable one. Rate constant value in aqueous medium was higher than in gas phase due to the energy stabilizing effect of water.

References

1. F. M. Oliveira, L. C. A. Barbosa, S. A. Fernandes, M. R. Lage, J. W. M. Carneiro and M. A. Kabeshov, *Comput. Theor. Chem.*, 2016, **1090**, 218.
2. F. M. Oliveira, L. C. A. Barbosa and F. M. D. Ismail, *RSC Adv.*, 2014, **4**, 18998.
3. M. Petric, M. Crisan, L. Crisan and G. Iltia, *Rev. Roum. Chim.*, 2015, **60**, 197.
4. I. K. Konstantinou, D. G. Hela and T. A. Albanis, *Environ. Pollut.*, 2006, **141**, 555.
5. T. A. Albanis, D. G. Hela, T. M. Sakellarides and I. K. Konstantinou, *J. Chromatogr. A*, 1998, **823**, 59.
6. G. Kovacevic and A. Sabljic, *Chemosphere*, 2013, **92**, 851.
7. B. Sun, A. V. Vorontsov and P. G. Smirniotis, *J. Hazard. Mater.*, 2011, **186**, 1147.
8. E. A. Kozlova, P. G. Smirniotis and A. V. Vorontsov, *J. Photochem. Photobiol. A*, 2004, **162**, 503.
9. A. V. Vorontsov, D. V. Kozlov, P. G. Smirniotis and V. N. Parmon, *Kinet. Catal.*, 2005, **46**, 189.
10. A. Vega-Rodriguez and J. Raúl Alvarez-Idaboy, *Phys. Chem. Chem. Phys.*, 2009, **11**, 7649.
11. B. Baidya, M. Lily and A. K. Chandra, *Comput. Theor. Chem.*, 2017, **1119**, 1.
12. A. Hatipoglu, D. Vione, Y. Yalçın, C. Minero and Z. Çinar, *J. Photochem. Photobiol. A*, 2010, **215**, 59.
13. S. Shah and C. Hao, *J. Environ. Sci.*, 2017, **57**, 85.
14. Gaussian 09, Revision A.02 Gaussian, Inc., Wallingford, CT, 2009.
15. A. D. Becke, *J. Chem. Phys.*, 1993, **98**, 5648.
16. C. Lee, W. Yang and R. G. Parr, *Phys. Rev. B*, 1988, **37**, 785.
17. J. Luo, X. Jia, Y. Gao, G. Song, Y. Yu, R. Wang and X. Pan, *J. Comput. Chem.*, 2010, **32**, 987.
18. X. Sun, C. Zhang, Y. Zhao, J. Bai, X. Zhang and W. Wang, *Environ. Sci. Technol.*, 2012, **46**, 8148.
19. Y. Takano and K. N. Houk, *J. Chem. Theory Comput.*, 2005, **1**, 70.

20. M. Kılıç and Z. Çınar, *J. Mol. Struct.-Theochem.*, 2008, **851**, 263.
21. C. Li, J. Chen, H. B. Xie, Y. Zhao, D. Xia, T. Xu, X. Li and X. Qiao, *Environ. Sci. Technol.*, 2017, **51**, 5043.
22. G. W. Wheland *J. Chem. Soc.*, 1941, **64**, 900.
23. Q. Zhang, X. Qu and W. Wang, *Environ. Sci. Technol.*, 2007, **41**, 6109,
24. I. N. Levine, "Physical Chemistry", 6th ed., ed. Tamara L. Hodge, McGraw Hill Higher Education, 2009, **22**, 892.